Fabrication of microfiltration membranes from polyisobutylene/polymethylpentene blends

Running title: Fabrication of membranes from polyisobutylene/polymethylpentene blends

Viktoria Y. Ignatenko, Tatyana S. Anokhina, Sergey O. Ilyin,* Anna V. Kostyuk,
Danila S. Bakhtin, Sergey V. Antonov, Alexey V. Volkov
A.V. Topchiev Institute of Petrochemical Synthesis, Russian Academy of Sciences
29 Leninsky prospect, 119991 Moscow, Russian Federation
*Corresponding author. E-mail: s.o.ilyin@gmail.com

The table of contents:

It is easy to obtain membrane precursors from polyisobutylene/polymethylpentene immiscible blends due to their low viscosity. Solvent extraction generates a microfiltration membrane.

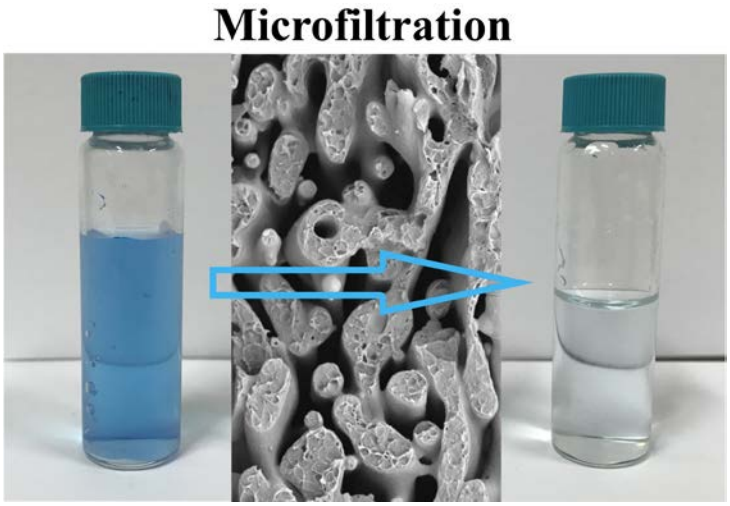

Abstract

An approach for fabrication of microfiltration membranes by solvent extraction of one of the immiscible components from polymer blend was developed. Poly(4-methyl-1-pentene) (PMP) was a membrane material, whereas poly(isobutylene) (PIB) was an extractable component. PIB content varied in the wide range of 0-45 wt.%, and all blends can be melted and processed at the temperature of 240°C. The rheological study demonstrated a pronounced non-Newtonian behavior of PMP/PIB blends and their very low viscosity due to interlayer slip. With PMP content of 55 and 60 wt.%, it was possible to fabricate the microfiltration membranes with water permeability of 31 and 3.7 m^3/m^2 h bar, respectively. The microfiltration membranes based on both compositions demonstrated good rejection performance on the level of 93-98% for

This article has been accepted for publication and undergone full peer review but has not been through the copyediting, typesetting, pagination and proofreading process which may lead to differences between this version and the Version of Record. Please cite this article as doi: 10.1002/pi.5932

submicron particles of phthalocyanine dye having the size 240 nm. These results allow concluding that PMP/PIB system can be utilized for fabrication of filtration membranes by means of 3D printing followed by solvent extraction.

Keywords: microfiltration, membranes, polyolefins, polymer blends, extraction, rheology

1. Introduction

Microfiltration is a pressure-driven process that allows separating the particles having the size of 0.1-1 micron (e.g., suspensions, large colloids, bacteria or microorganisms).[1,2] This separation technique is widely used in the pharmaceutical, food, petrochemical, textile industries, as well as in medicine, electronics, biotechnology, and for both industrial and domestic wastewater purification.[3] Besides, microfiltration membranes can be considered as a porous support for the fabrication of thin-film composite membranes[4] or liquid membranes.[5-7] The microfiltration membranes are commonly made of both hydrophobic and hydrophilic polymers such as polytetrafluoroethylene,[8,9] polyvinylidene fluoride,[10] polyolefines,[11-14] cellulose ethers,[15-17] polycarbonates,[18,19] polyamides,[20,21] polyetheretherketone,[22] polysulfone and polyethersulfone,[23-25] and polyimides.[26] The porous structure of polymeric microfiltration membranes is usually formed by the polymer precipitation in the coagulation bath (phase inversion),[27-30] etching of the tracks after polymer film bombarding by heavy ions,[31,32] polymer crazing,[33] and extraction/decomposition of another component in the polymer matrix.[34]

The recent progress in the development of different types of 3D-printing techniques provides a new powerful tool for fabrication of tailor-made membranes and compact membrane devices.[35-38] In return, it requires further study on the optimization of polymer composition suitable for processing in 3D printers in order to increase the range of membrane materials and membranes fabricated by such way. The most widely used, developed and economically feasible approach is the layer-by-layer printing using the melted polymeric material. However, the current level of available technologies in this area does not allow direct arrangement of the regular porous structure even for microfiltration range. Therefore, we are currently developing the approach that allows combining the advantages of 3D printing and microphase separation in the polymeric system. In this proposed concept, 3D printing of the polymeric composition consisting of at least two polymers or a polymer and a low-molecular-weight component precisely sets the membrane geometry. The porous structure of the resulted membrane is arranged by selective extraction of one component by any means, while the remained polymer forms the porous carcass of the membrane.

In order to form the porous membranes in this way, the polymeric systems consisting of at least two components shall be: i) immicible at room temperature to form heterogeneous

system with the microphase separation, ii) suitable for hot-melt processing, iii) thermally stable at processing conditions, iv) have acceptable viscosity, v) have different nature that allows selective extraction of one component, while other polymeric material would preserve its pre-settled structure, vi) possess good mechanical properties, vii) preferably, easy to clean out from the equipment.

Previously, similar approach was used to obtain porous polymers, e.g., from a mixture of polystyrene with polylactide,[39] polyethylene with poly(ethylene oxide),[40] chitosan with poly(vinyl pyrrolidone) or poly(ethylene oxide),[41,42] polyolefin with polystyrene,[43] and polypropylene with polybutene.[44] However, in most of these studies, the authors only showed the possibility of obtaining membrane structure, but did not investigate transport properties of resulting materials. In this research, we have selected the system consisting of poly(4-methyl-1-pentene) (PMP) and polyisobutylene (PIB) that meets these criteria.[45] Due to its low energy of intermolecular interactions, PMP possesses some properties similar to polytetrafluoroethylene, including good chemical resistance, inertness, and biocompatibility.[14,46,47] At the same time, the high melting point of PMP (T_m = 237°C) allows processing of this polymer with the conventional approaches and withstanding high temperature sterilization if required.[48,49] As a result, PMP-based microfiltration membranes are considered for both medical (e.g., filtration of blood plasma)[50,51] and food applications (e.g., dairy production).[52,53]

The goal of this work was to fabricate the flat-sheet microfiltration membranes by hot-melt processing of the dual polymer mixture with the different PMP/PIB ratio followed by the extraction of PIB to form a porous structure of the resulted membranes. The optimized polymeric composition can be considered for further fabrication of filtration membranes using the 3D printing technique. It is important to note that, except the last stage of extraction of PIB, no solvent would be required for fabrication of PMP/PIB rod and printing of the membrane that makes this approach environmentally oriented one.

2. Experimental

2.1. Materials and membrane fabrication

Poly(4-methyl-1-pentene) (TPX MX004; Mitsui Chemicals, Japan) having MFI = 25 g/(10 min) with 5 kg load at 260°C and polyisobutylene (Oppanol B15; BASF, Germany) having

M_w = 1.08x10^5 g/mol and M_w/M_n = 3.2 were used in this study. Different compositions with PMP/PIB weight ratio of 55/45, 60/40, 65/35, 75/25, 85/15, and 95/5 were prepared by using HAAKE Polydrive twin-rotor mixer equipped with sigma-blade rotors (1 hour at 240°C with rotation speed of 30 rpm (approx. 25 s^{-1})).

The membrane precursor films with the thickness of 50 ± 10 μm were fabricated by using HLCL-1000 laminator (ChemInstruments, USA) by placing the polymer blend between two layers of a silicone-treated anti-adhesive polyimide film at a temperature of 240°C. The membranes were allowed to cool down to ambient conditions and then were immersed in heptane for 24 hours to wash out PIB from PMP matrix. The membranes were placed then in another bath with heptane for 2 hours with following drying at ambient conditions. At each stage, the weight of membrane samples was controlled. As a result, PMP films were obtained whose transparency decreased with increasing concentration of the extracted PIB (Figure 1): the films prepared from blends with 5-15% of PIB were practically transparent, whereas those prepared from ones with a higher PIB concentration were almost opaque.

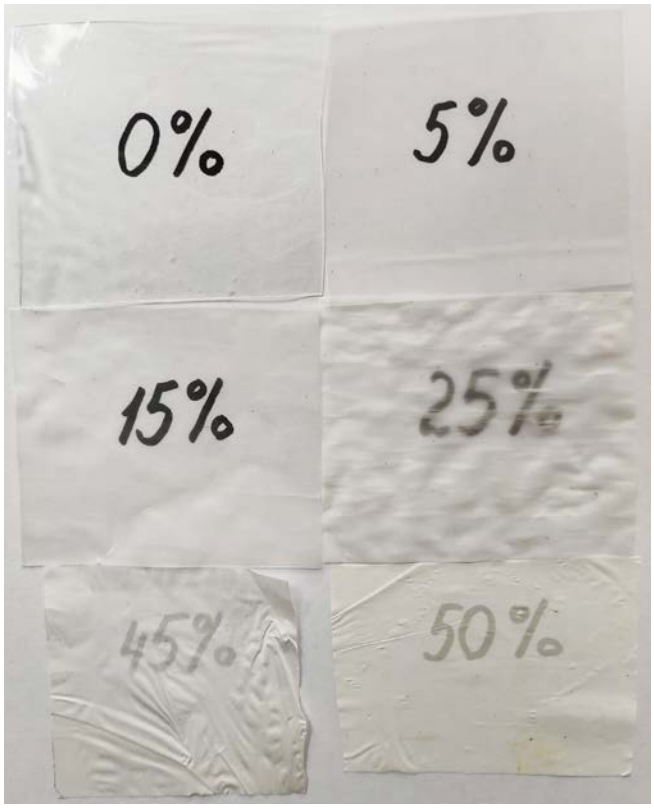

Figure 1. Photograph of membranes obtained by removing polyisobutylene from its mixture with polymethylpentene. The membranes were placed on a paper on which the initial content of PIB was written.

2.2. Characterization methods

Differential scanning calorimetry was carried out by using a MDSC 2920 calorimeter (TA Instruments, USA) within the temperature range from -30 to 270°C at the heating or cooling rate of 10°C/min.

The rheological properties of PMP/PIB blends were studied with a DHR-2 rotational rheometer (TA Instruments, USA) at 240°C using a cone–plate unit (25 mm diameter, 2°). The following deformation modes were applied for samples characterization: i) steady-flow with the stepwise increase of shear rate from 0.0001 to 100 s^{-1}; ii) small amplitude oscillatory shear with the stepwise decrease of angular frequency from 628 to 0.0628 s^{-1} at a constant strain amplitude of 0.1%.

Microphotographs of mixtures placed between two cover glasses were taken at 25°C using an objective with 3.5× magnification and a digital camera with 12MP 1/1.7"-type Sony IMX226 CMOS image sensor.

Tensile tests of PMP membranes (60 mm length, 10 mm width) were performed with TT-1100 machine (ChemInstruments, USA) at 25°C and a constant speed of 3.8 cm/min.

The change in the film morphology upon the extraction of PIB was visualized by analysis of the cross-section of the membrane by a TM-3030Plus scanning electron microscope (Hitachi, Japan). For this purpose, the samples were broken in the liquid nitrogen and covered by ~50 Å gold coating. SEM images of film surfaces were processed on the Gwyddion software (Czech Metrology Institute) to determine the surface porosity.

2.3. Filtration experiments

The filtration experiments were carried out at room temperature and pressure of 1 bar in a setup with a dead-end filtration cell (active service area is about 3.14 cm^2) equipped with a stirring system. The performance of the membranes was characterized in terms of liquid permeability coefficient P [kg/m^2hbar]. For retention experiments, a aqueous dispersion of phthalocyanine particles with a size of 240 nm and a concentration of 0.01 wt.% was used. The

disperse phase concentrations in the feed and permeate were determined using an UV–vis spectrometer PE-5400UV (Ecroskhim, Russia) at a wavelength of 600 nm. The retention coefficient was calculated as follows:

$$R(\%) = \left(1 - \frac{C_p}{C_f}\right) \cdot 100\%$$

where C_p and C_f are the phthalocyanine concentrations in the permeate and the feed, respectively.

3. Results and discussion

3.1. Properties of PMP/PIB mixtures

According to DSC data (Figure 2), the introduction of 5 wt.% of PIB in PMP led to the decrease of melting point as well as to the increase of crystallization temperature and the crystallinity of PMP (Table 1). Further increasing of PIB content in PMP/PIB mixture does not change either the melting point or the crystallization temperature. This suggests that a part of the PIB (but not more than 5 wt. %) was dissolved in the PMP medium. With the increase of PIB concentration, the drop in the enthalpies of melting and crystallization of PMP/PIB mixture was observed, which can be attributed mainly to the decrease in the content of the component capable of crystallization. At the same time, the enthalpies of crystallization and melting of PMP in PMP/PIB mixture were somewhat higher than those calculated from the value of the neat PMP and its content in the blends as can be noticed from Figure 3. However, the maximum difference in the melting temperature of PMP in the polymer mixture with PIB (with concentration up to 55 wt.%) did not exceed 4.4°C; therefore, these materials can be processed nearly at the same operating conditions regardless of their composition.

As a result of immiscibility, PIB forms an emulsion-like composite in the matrix of PMP. The inspection of PMP/PIB thin films did not reveal PIB drops within PMP matrix at low PIB content (likely, their sizes were smaller than 1 μm). However, the increase of PIB loading resulted in the formation of visible microphase in the PIB matrix (see micrograph of 50 wt.% PIB in Figure 4).

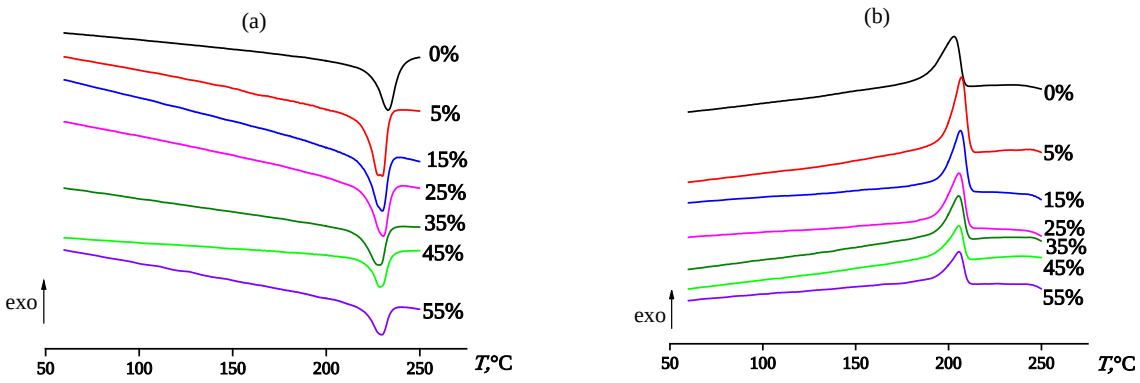

Figure 2. Thermograms of PMP/PIB mixtures at different PIB content: heating (a) and cooling (b) scans at 10°C/min.

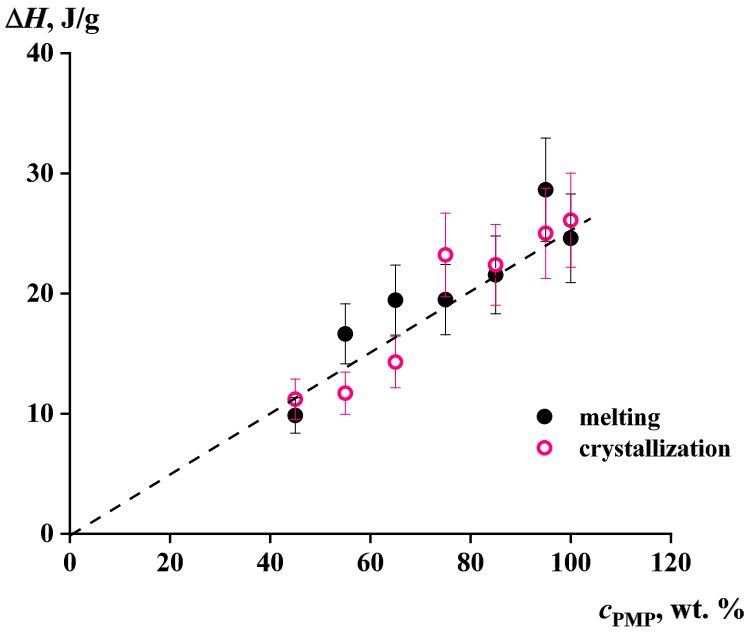

Figure 3. Enthalpy of melting and crystallization of PMP/PIB mixture as a function of PMP concentration. The theoretical enthalpy of melting of PMP in PMP/PIB mixture is given as the dotted line.

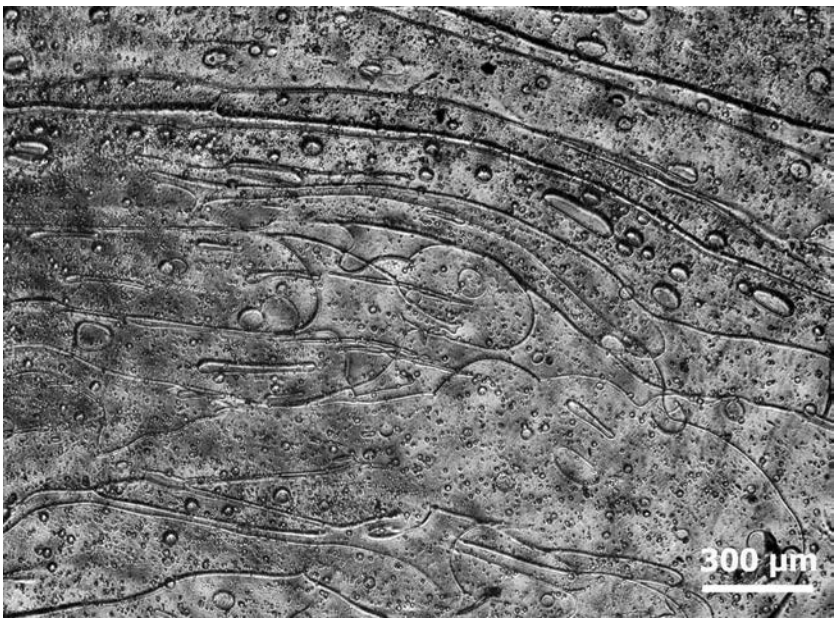

Figure 4. A micrograph of PMP/PIB mixture with PIB content of 50 wt.% at 25°C before PIB extraction.

The viscosity of the melted mixture can play an important role in the formation of the 3D architecture of the resulting films. Bearing this in mind, the rheological properties of PMP, PIB, and their blends were studied at the temperature of 240°C. For better visualization, the data for PMP/PIB mixtures were divided into two graphs showing the results for polymer blends containing 5-35 wt.% (Figure 5a) and 40-50 wt.% of PIB (Figure 5b); the data for neat PMP and PIB are given in both figures. As can be seen, the polymeric systems studied in this research acted as non-Newtonian fluids. At low stresses, the viscosity of both polymers did not depend on shear stress, whereas the drop in the viscosity was observed at higher stresses. The viscosity of neat PMP (17000 Pa·s) was noticeably greater the corresponded value for PIB (340 Pa·s). It is interesting to note that at the certain stresses, the viscosity of all PMP/PIB mixtures was lower than for neat PIB.

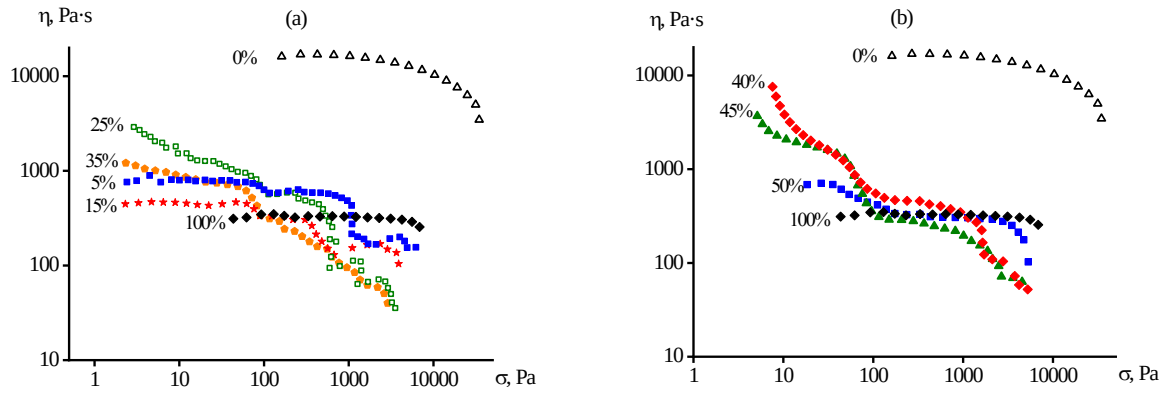

Figure 5. Flow curves of PMP/PIB blends at different PIB content at 240°C. Captions at curves indicate the PIB content in the blends.

The addition of 5 wt.% of PIB to PMP matrix resulted in the dramatic drop in the viscosity of composite material compared with the neat PMP. The viscosity of this material did not comply with the rule of logarithmic additivity of the viscosity of PMP and PIB with the respect of their content. The sharp decrease in the viscosity with the addition of PIB could be explained by interlayer slip[54] instead of the homogeneous flow of the sample during deformation. The viscosity of the blends remains approximately at the same level with a further increase of PIB content.

The surface tensions of PIB and PMP are 31.8 and 24 mN/m, respectively. Based on this, according to Antonow's rule,[55] the interfacial tension at the boundary of two polymers can be estimated as 7.8 mN/m. The contact angle formed by a PIB drop on the surface of the PMP film equal to 60°. Thus, according to the Young–Dupré equation, work of adhesion of PIB to PMP can be estimated as 0.012 J/m^2. Such low adhesion of two polymers can lead to sliding of their phases relative to each other during deformation of the mixture. Hence, a large scattering of the experimentally measured viscosity values and absence of correlation between PIB content and viscosity of the mixture are due to the instability of the flow accompanied by an interlayer slip. In addition, it is impossible to exclude a macroscopic slip of the sample over a thin PIB layer at the measuring surface. In our case, as a result of the rheological tests, some effective (apparent) viscosity of the blends was measured.

Quite surprisingly, the introduction of 40–45% of PIB leads to a significant increase in the apparent viscosity of the mixtures in the region of low shear stresses, which can be explained

by the presence of the yield stress.[56] Probably, at 40% PIB content in the mixture, a certain transition was observed: from the structure of PIB-in-PMP emulsion to gyroid-like structure[57] of bicontinuous phases of PIB and PMP. At the deformation of samples, coarse-grained mixtures enriched with PIB form extended continuous phases (see Figure 4) on the surface of which the slip occurs. The gyroid-like structure was confirmed by the cross-section SEM image of the sample after PIB extraction (Figure 6e).

With PIB content in PMP/PIB mixture increasing up to 50%, the yield stress disappears due to the transition from gyroid-like structure to the PMP-in-PIB emulsion, and the viscosity of the mixture in the region of moderate shear stresses equal to that of pure PIB. SEM analysis of the cross-section revealed that the sample possessed a fibrous structure, and the fibers did not merge with each other, unlike in the case of the formation of gyroid-like structure. At high shear stresses, the apparent viscosity of all the blends is lower than the viscosity of both polymers due to an interlayer slip; similar behavior is typical for mixtures of components with poor adhesion, e.g., for polyethylene and boric acid blends.[58] It should be noted that the preparation of all the blends occurred using a high shear rate (25 s^{-1}), which thus provided the interlayer slip. It is impossible to precisely measure the effective viscosity of the blends under such conditions on a rotary rheometer; suggesting that the viscosity did not exceed 100 Pa·s.

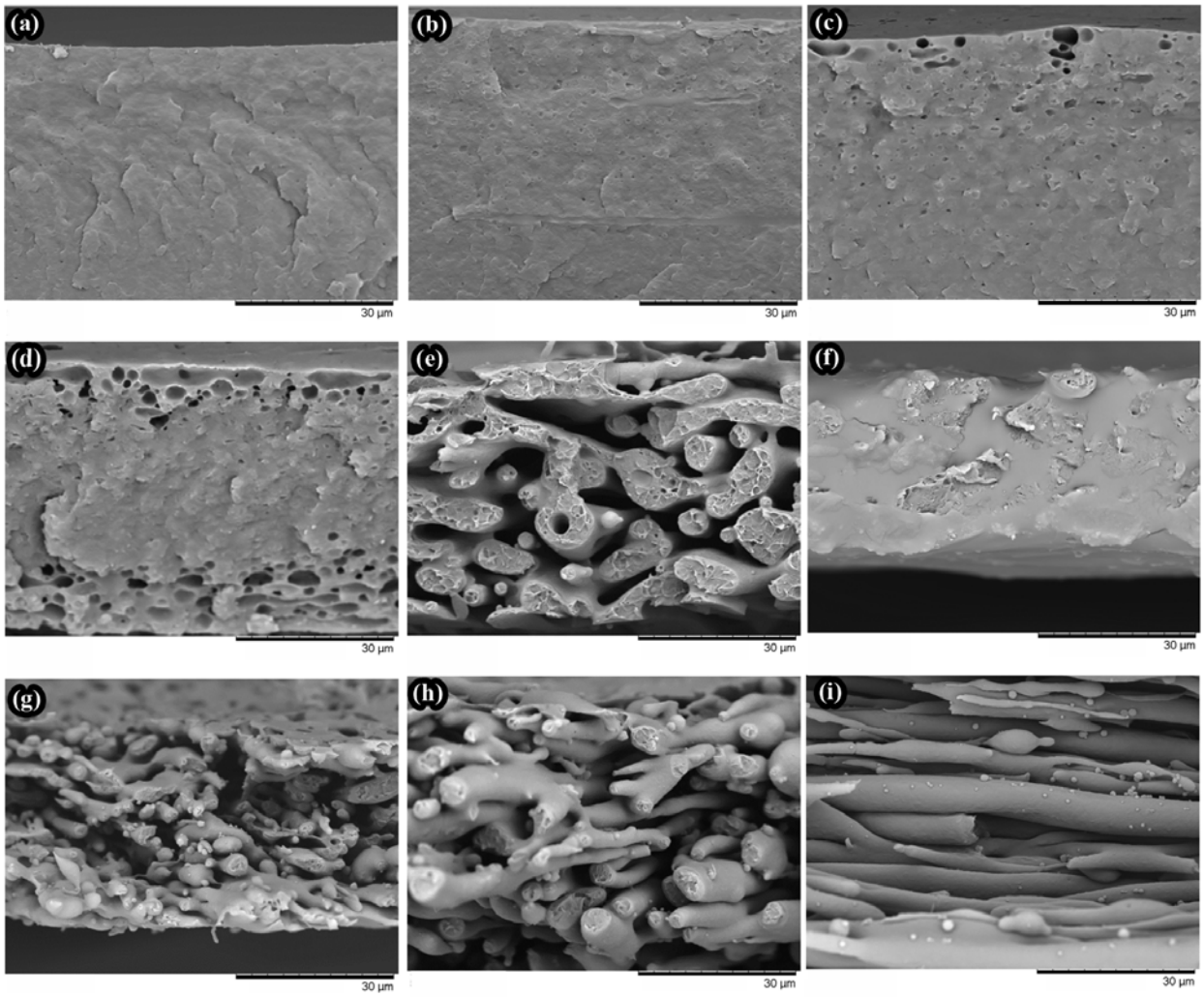

Figure 6. SEM images of cross-sections of PMP films before (f) and after (a–e, g–i) PIB extraction: 5 (a), 15 (b), 25 (c), 35 (d), 40(e), 45 (f, g), 50 (h), 55 (i) % of PIB. The lengths of the black lines located in the lower right corners of the images correspond to 30 μm.

The nature of the dispersion medium affects the viscoelastic properties of the resulting material. Initially, the pure polymers acted like typical Maxwell liquids: at the low-frequency region, $G' \sim \omega^2$ and $G'' \sim \omega$ (Figure 7). The slope of the storage modulus of PIB-in-PMP emulsion (as well as of the sample with bicontinuous morphology) is equal to 1.0, which could be explained by the expansion of the sample relaxation time spectrum due to the limited dissolution of PIB in PMP with the corresponding widening of the molecular weight distribution of the continuous medium.[59,60] The bicontinuous blend has a behavior intermediate between

those of a viscous fluid and an elastic solid due to its preliminary squeezing between the cone and the plane; after annealing, for such blends is typical solid-like behavior.[61] For PMP-in-PIB emulsion, dependences of storage and loss moduli showed the similar slope as for the pure PMP and PIB. This confirmed the fact that PMP was not soluble in PIB at all. It should be noted that for immiscible polymer blends, there is a contribution of interfacial relaxation to the total viscoelasticity.[62,63] However, for these blends this contribution is negligible due to the low interfacial tension. By way of example, if interfacial relaxation has an effect, then $G''(\omega)$ curve of the blends should be at least higher than the one of PIB, and $G'(\omega)$ curve of the bicontinuous blend should become less sloping with decreasing frequency;[64] these are not observed.

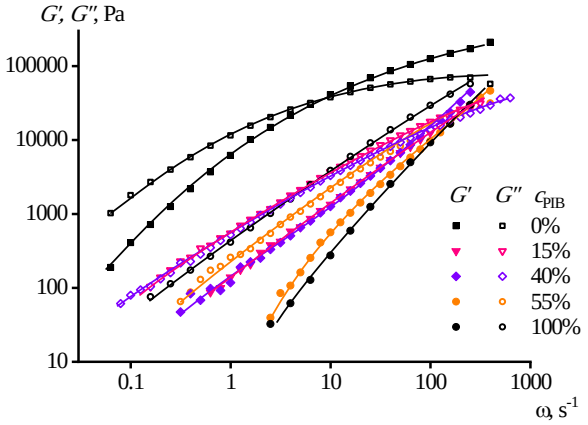

Figure 7. Frequency dependences of the storage and loss moduli of PMP/PIB mixtures at 240°C.

3.2. Filtration properties of PMP-based membranes

The concentration of PIB in PMP/PIB films was in the range from 0 up to 55 wt.%. As can be seen from the data on weight loss at PIB extraction presented in Table 2, it was possible to extract most of PIB from the PMP/PIB blends by two-step washing in heptane bath. It is surprising that the extraction was complete even in the case of low PIB content which does not lead to the formation of open pores. The explanation may lie in the fact that most of PIB was concentrated near the surface of the film. This is evidenced by the presence of near-surface voids (with sizes of 1-4 μm) in the samples initially containing 25 and 35% of PIB which was then extracted (Figures 6c and 6d). The concentration of PIB near the surface (as well as its uneven distribution) may explain the low apparent viscosity of the blends with a small proportion of this

less-viscous polymer. It remains unclear whether such uneven distribution is caused by poor mixing and/or by the procedure of forming films by squeezing on the rolls.

Due to the extraction of PIB from the blends, they underwent a slight contraction (no more than 2-5% according to film length contraction, see also Figures 6f and 6g); nevertheless, all membrane samples with initial PIB content of 35 wt.% or lower have the negligible surface porosity (see Table 2). The study of mechanical properties revealed a noticeable increase in the tensile strength and elongation at break of resulted films after extraction when the content of PIB was 5 wt.% (Figure 8). On the one hand, it can be attributed to the fact that PIB possessed limited solubility in PMP and some residue of PIB can remain in PMP matrix acting as a plasticizer, e.g., PMP melting point depression takes place (see Table 1). As a result, the elasticity of the films increases. On the other hand, the addition of PIB increases the crystallinity degree of PMP and its crystallization temperature, perhaps due to ability of small PIB droplets and voids remaining after PIB extraction act as nucleation centers. This increase in crystallinity improves the film strength. However, further increase of PIB leads to a two-phase structure that facilitates quantitative extraction and formation of a porous structure, but resulted in the decrease of mechanical properties with the increase of PIB content in the initial blend.

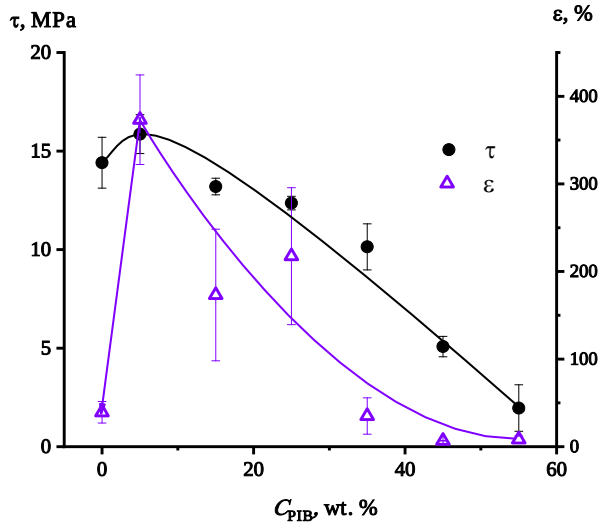

Figure 8. Tensile strength and elongation at break of membranes as a function of PIB content in the initial PMP/PIB film.

As can be seen from Table 2, the decrease of PIB concentration from 45 to 40 wt.% led to the drop in the surface porosity of the membranes but less than twice, while the water

permeability coefficient decreased by one decimal order of magnitude. The decrease in the amount of pores leads to a decrease in the flow of water passing through the membrane.[34] The surface porosity is proportional to the square of the effective radius of pores (or even to a smaller fractional number in the case of pore merging) whereas the permeability is proportional to the fourth degree of their radius according to the Hagen-Poisell law. The decrease in the concentration of PIB by another 5 wt. % led to a dramatic decline in the surface porosity and was associated with the decrease in water permeability for more than 200 times. With a further decrease of PIB concentration, the films became a barrier for the water and it was not possible to experimentally detect the liquid flow across the membrane even when the trans-membrane pressure was increased from 1 up to 20 bar. Indeed, the analysis of the cross-section of different samples visualized by SEM revealed that the interconnected porous structure (with maximum pore sizes of 1-8 μm) was found only in the case of PIB concentration of 35 wt.% or higher (see Figure 6e, 6g, and 6h). At lower PIB concentration, the microvoids especially in the sub-surface layer can be found, but there is no evidence of the existence of the percolation porous structure required for the establishment of liquid transport across the membrane (see Figure 6a-6d).

To evaluate the separation performance, the membranes prepared by PIB extraction from PMP/PIB blends with PIB concentration of 40 and 45 wt.% in the initial mixture were tested for the rejection of submicron particles of phthalocyanine dye having the average hydrodynamic diameter of 240 nm. Both samples demonstrated good rejection performance of 90+%, with the increase of PMP concentration from 55 to 60% leading to a slight increase of the rejection from 93 to 98%. The samples of the feed and permeate are shown in Figure 9. To sum up, it was possible to fabricate microfiltration membranes that enable to separate the solutes with the size particle size from 0.2 μm. However, it was not possible to prepare the tighter membranes with ultra- or nanofiltration range by an increase of PMP concentration in the initial polymer blend due to the collapse of porous structure at the stage of extraction and drying. The further optimization of the polymeric composition is still required.

The formation of morphology is influenced by the interfacial tension and the ratio between the viscosities of two phases. Both factors influence the size of the emulsion droplets and, accordingly, the future pore size. The optimal ratio of viscosity of disperse phase to that of continuous phase for drop breaking is 0.1-1.[65] This range of viscosity ratio allows one to break

drops at lower shear rates. In our case, the viscosity ratio is slightly lower (0.02), but its increase would not change anything because of the used high mixing rate. However, the interfacial tension (more precisely the capillary number) affects lifetime of polymer threads formed during mixing.[66] In a case of low interface tension, extended threads are formed and structure of a blend is determined by the thread-thread coalescence and independent of composition; pore size is determined by the proximity of the viscosity of the polymers. In a situation of high interfacial tension (as in our case), the structure is determined by droplet-droplet coalescence: pore continuity appears only at a certain concentration of a dispersed phase and pore sizes increase with their proportion. Thus, to reduce the pore size, use of an amorphous component of less interfacial tension with polymethylpentene or addition a compatibilizer is necessary. In the case of using a compatibilizer, such as a copolymer, the structure is still determined by the coalescence of the droplets rather than the threads, but the pore size is significantly lower.[67]

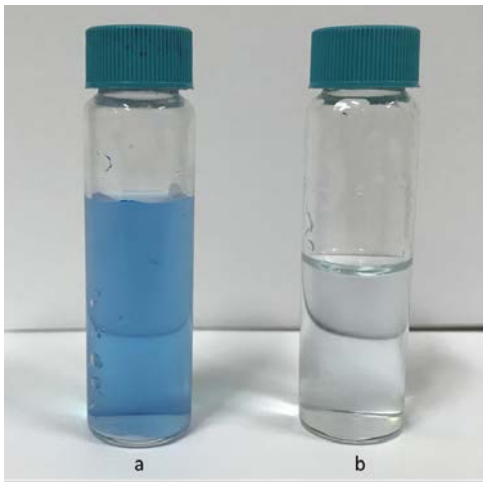

Figure 9. Image of an aqueous dispersion of phthalocyanine before (a) and after filtration (b).

4. Conclusion

In this research, a new approach for fabrication of microfiltration membranes by the hot-melt processing of two-component polymer blend based on poly(4-methyl-1-pentene) and poly(isobutylene) followed by the extraction of the amorphous component with heptane were proposed. The rheological study demonstrated that addition even 5% of PIB to PMP results in a more than tenfold decrease in its viscosity due to low adhesion between the polymers leading to interlayer slip. At the same time, the introduction of 40–45 wt.% of PIB (but less than 50%) leads to a significant increase in the viscosity of the mixture in the region of low shear stresses,

which can be explained by the presence of yield stress in these samples. Apparently, with increasing concentration of PIB in the mixture, a transition occurs from the structure of PIB-in-PMP emulsion to the gyroid-like structure of bicontinuous phases, and then to PMP-in-PIB emulsion. The PMP structure formed in the molten mixture persists when the mixture is cooled and PIB is washed out. Thus, due to the immiscibility of PMP and PIB resulted in two-phase morphology, it is possible to form a porous structure inside the PMP matrix by selective solvent extraction of PIB. However, due to high interfacial tension in PMP/PIB blends, it was not possible to obtain interconnected porous structure inside the membrane matrix when PMP concentration in the blend was 75 wt.% or greater. In the case of lower PMP content (55-60 wt.%), it was possible to fabricate the microfiltration membranes with good combination of dispersion-medium permeability and submicron-particle rejection performance. The low viscosity of PIB/PMP blends makes it possible to extrude them by using of precision 3D printer for formation of complex-profile products, and the complete extractability of PIB makes it simply to convert these products to membranes. However, the additional studies are required for further optimization of the composition of the polymeric matrix and extraction process that would enable the fabrication of tighter membranes within ultra- or nanofiltration range.

Acknowledgments: This research was supported by the Council for Grants of the President of the Russian Federation [grant number MD-6642.2018.8].

References

1 Van Der Bruggen B, Vandecasteele C, Van Gestel T, Doyenb W and Leysenb R, *Environ Prog* **22**:46-56 (2003).

2 Cassano A and Basile A, *Energy Environ Appl*: 647-679 (2011).

3 L.J. Zeman LJ and Zydney AL, *Microfiltration and ultrafiltration: Principles and applications* (2017).

4 Bazhenov SD, Borisov IL, Bakhtin DS, Rybakova AN, Khotimskiy VS, Molchanov SP et al., *Green Energy Environ* **1**: 235-245 (2016).

5 Fortunato R, Afonso CAM, Benavente J, Rodriguez-Castellón E and Crespo JG, *J Memb Sc.* **1**:235-245 (2005).

6 Akhmetshina AA, Davletbaeva IM, Grebenschikova ES, Sazanova TS, Petukhov AN, Atlaskin AA et al., *Membranes* **6**:4 (2015).

7 Akhmetshina AA, Yanbikov NR, Petukhov AN and Vorotyntsev IV, *Pet Chem* **57**:770-778 (2017).

8 Yoo H and Kwak SY, *J Memb Sci* **448**:125-134 (2013).

9 Mo D, Liu JD, Duan JL, Yao HJ, Latif H, Cao DL et al., *Nucl Instrum Methods Phys Res Sect B* **333**:58-63 (2014).

10 Liu J, Li P, Li Y, Xie L, Wang S and Wang Z, *Desalination* **249**:453-457 (2009).

11 Salam A and Ulbricht M, *Macromol Mater Eng* **292**:310-318 (2007).

12 Dickson JM, Childs RF, McCarry BE and Gagnon DR, *J Memb Sci* **148**:25-36 (1998).

13 Al-Obeidani SKS, Al-Hinai H, Goosen MFA, Sablani S, Taniguchi Y and Okamura H, *J Memb Sci*, **307**:299-308 (2008).

14 US4415608 Continuous production of polymethylpentene membranes (1983).

15 Sossna M, Hollas M, Schaper J and Scheper T, *J Memb Sci* **289**:7-14 (2007).

16 Hashino M, Hirami K, Katagiri T, Kubota N, Ohmukai Y, Ishigami T et al., *J Memb Sci* **379**:233-238 (2011).

17 Ritchie SMC, Bachas LG, Olin T, Sikdar SK and Bhattacharyya D, *Langmuir* **15**:6346-6357 (1999).

18 Bowen WR and Cooke RJ, *J Colloid Interface Sci* **15**:280-287 (1991).

19 Tracey EM and Davis RH, *J Colloid Interface Sci* **167**:104-116 (1994).

20 Vasileva N and Godjevargova T, *J Memb Sci* **239**:157-161 (2004).

21 Han J, Meng S, Dong Y, Hu J and Gao W, *Water Res* **47**:197-208 (2013).

22 Sonnenschein MF, J *Appl Polym Sci* **72**:175-181 (1999).

23 Ohya H, Shiki S and Kawakami H, *J Memb Sci* **326**:293-302 (2009).

24 Susanto H, Stahra N and Ulbricht M, *J Memb Sci* **342**:153-164 (2009).

25 Ulbricht M, Schuster O, Ansorge W, Ruetering M and Steiger P, *Sep Purif Technol* **57**:63-73 (2007).

26 Eastmond GC, Gibas M, Pacynko WF and Paprotny J, *J Memb Sci* **207**:29-41 (2002).

27 Ilyin SO, Makarova VV, Anokhina TS, Ignatenko VY, Brantseva TV, Volkov AV and Antonov SV, *Cellulose* **25**:2515-2530 (2018).

28 van de Witte P, Dijkstra PJ, van den Berg JWA and Feijen J, *J Memb Sci* **117**:1-31 (1996).

29 Tanakaa T and Lloyd DR, *J Memb Sci* **238**:65-73 (2004).

30 Ilyin SO, Makarova VV, Anokhina TS, Volkov AV and Antonov SV, *Polym Sci Ser A* **59**:676-684 (2017).

31 Apel P, *Radiat Meas* **34**:559-566 (2001).

32 He D, Susanto H and Ulbricht M, *Progr Polym Sci* **34**:62-98 (2009).

33 Sadeghi F, Ajji A and Carreau PJ, *J Memb Sci* **292**:62-71 (2007).

34 Mulder M, Basic Principles of Membrane Technology. Second edition. (1997).

35 Fritzmann C, Hausmann M, Wiese M, Wessling M and Melin T, *J Memb Sci* **446**:189-200 (2013).

36 Femmer T, Kuehne AJC and Wessling M, *Lab Chip* **14**:2610-2613 (2014).

37 Femmer T, Kuehne AJC, Torres-Rendon J, Walther A and Wessling M, *J Memb Sci* **478**:12-18 (2015).

38 Lee JY, Tan WS, An J, Chua CK, Tang CY, Fane AG et al., *J Memb Sci* **499**:480-490 (2016).

39 Esquirol AL, Sarazin P and Virgilio N, *Macromolecules* **47**:3068-3075 (2014).

40 Trifkovic M, Hedegaard A, Huston K, Sheikhzadeh M and Macosko CW, *Macromolecules* **45**:6036-6044 (2012).

41 Zeng M, Fang Z and Xu C, *J Membr Sci* **230**:175-181 (2004).

42 Zeng M, Fang Z and Xu C, *J Appl Polym Sci* **91**:2840-2847 (2004).

43 US4868222 Preparation of asymmetric membranes by the solvent extraction of polymer components from polymer blends (1989).

44 Matsuyama H, Okafuji H, Maki T, Teramoto M and Tsujioka N, *J Appl Polym Sci* **84**:1701-1708 (2002).

45 Anokhina TS, Ilyin SO, Ignatenko VY, Bakhtin DS, Kostyuk AV, Antonov SV and Volkov AV *Polym Sci Ser A* **61**:619-626 (2019).

46 Rambaud J, Guilbert J, Guellec I and Renolleau S, *Perfusion* **28**:14-20 (2012).

47 Lehle K, Friedl L, Wilm J, Philipp A, Müller T, Lubnow M et al., *Artif Organs* **40**:577-585 (2016).

48 Rosenberg U and Bogl W, *Food Techn* **41**:92-99 (1987).

49 Rutala WA and Weber DJ, *Emerg Infect Dis* **7**:348-353 (2001).

50 Walker AK, *Anaesthesia* **33**:35-40 (1978).

51 Guidoin R, Domurado D, Poignant S, Gosselin C and Awad J, *Res Exp Med* **171**:129-139 (1977).

52 Pafylias I, Cheryan M, Mehaia MA and Saglam N, *Food Res Int* **29**:141-146 (1996).

53 Papadatos A, Neocleous M, Berger AM and Barbano DM, *J Dairy Sci* **86**:1564-1577 (2003).

54 Utracki LA, *J Rheol* **35**:1615-1637 (1991).

55 Antonow GN, *J Chim Phys* **5**:372-385 (1907).

56 Malkin A, Kulichikhin V and Ilyin S, *Rheol Acta* **56**:177-188 (2017).

57 Hajduk DA, Harper PE, Gruner SM, Honeker CC, Thomas EL and Fetters LJ, *Macromolecules* **28**:2570-2573 (1995).

58 Ilyin SO, Malkin AY, Kulichikhin VG, Shaulov AY, Stegno EV, Berlin AA et al., *Rheol Acta* **53**:467-475 (2014).

59 Brantseva T, Antonov S, Kostyuk A, Ignatenko V, Smirnova N, Korolev Y, Tereshin A and Ilyin S, *Eur Polym J* **76**:228-244 (2016).

60 Ilyin SO, Arinina MP, Polyakova MY, Kulichikhin VG and Malkin AY, *Fuel* **186**:157-167 (2016).

61 Rotella C, Tencé-Girault S, Cloitre M and Leibler L, *Macromolecules* **47**:4805-4812 (2014).

62 Graebling D, Muller R and Palierne JF *Macromolecules* **26**:320-329 (1993).

63 Gramespacher H and Meissner J, *J Rheol* **36**:1127-1141 (1992).

64 Yu W, Zhou W and Zhou C, *Polymer* **51**:2091-2098 (2010).

65 Grace HP, *Chem Eng Commun* **14**:225-277 (1982).

66 Willemse RC, Ramaker EJJ, Van Dam J and De Boer AP, *Polymer* **40**:6651-6659 (1999).

67 Li J, Ma PL and Favis BD, *Macromolecules* **35**:2005-2016 (2002).

Table 1. PIB/PMP mixtures: temperatures T and enthalpies ΔH of melting and crystallization.

PIB concentration,%	Melting		Crystallization	
	T_m, °C	ΔH_m, J/g	T_{cr}, °C	ΔH_{cr}, J/g
0	233.0	24.6	202.9	26.1
5	229.9	28.6	206.9	25.0
15	229.9	21.6	206.3	22.4
25	230.5	19.5	205.6	23.2
35	228.7	19.5	205.3	14.3
45	228.6	16.6	205.4	11.7
55	229.5	9.85	205.9	11.2

Table 2. Weight loss after extraction of PIB from PMP/PIB films, surface porosity, and water permeability for the resulted membranes.

PIB concentration, wt. % / vol. %	Weight loss after extraction, %	Surface porosity, %	Permeability P, kg/m^2 h bar
55 / 57.4	55.5	44.6	>100000
50 / 52.5	50.1	41.0	>100000
45 / 47.5	47.9	42.6	31000
40 / 42.4	41.0	26.0	3720
35 / 37.3	32.9	1.3	0.06
25 / 26.9	23.2	0.5	barrier
15 / 16.3	12.5	0.3	barrier
5 / 5.5	4.6	0.05	barrier
0 / 0	0	0	barrier